archives
of thermodynamics
Vol. **41**(2020), No. 4, 63–92
DOI: 10.24425/ather.2020.135854

Light extinction and ultrasound method in the identification of liquid mass fraction content in wet steam

MIROSŁAW MAJKUT*
SŁAWOMIR DYKAS
KRYSTIAN SMOŁKA

Department of Power Engineering and Turbomachinery,
Silesian University of Technology,
Konarskiego 18, 44-100 Gliwice, Poland

Abstract Recently, significant progress has been made in experimental studies on the flow of wet steam, measuring techniques based on recording the phenomenon of extinction of light and ultrasound have been elaborated or improved. The basic value experimentally determined in the final stage was the content of the liquid phase defined as the wetness fraction. The methodology of tests and experimental investigations was presented, as well as the applied and developed measurement systems. Next, some developed designs of new ultrasonic and light extinction measuring probe and their modifications are described. The article presents also some examples of applications of the developed measurement techniques in application to experimental research conducted on wet steam. Examples of comparison between experimental and numerical tests for the extinction method are also provided.

Keywords: Wet steam; Light extinction; Ultrasound method; Mass fraction content

Nomenclature

g	–	extinction coefficient
p	–	pressure, kPa
t	–	temperature, °C

*Corresponding Author. Email: miroslaw.majkut@polsl.pl

x – dryness, $= 100\% - y$
y – wetness mass fraction, %
c – speed of sound, ms
m – mass, kg
D_{32} – is the Sauter diameter, m
N – number of particles
Cv – volume fraction of droplets,
n – refractive index
D – diameter, m
I_0 – referential light intensity, AU
I_e – source light intensity, AU
I – light intensity, AU
L – distance, m
Q_{ext} – extinction coefficient from Mie theory
Q_a – absorption coefficient
Q_s – scattering coefficient
r – particle radius, m
X – scattering particle size
t – time, s

Greek symbols

λ – wavelength of the incident radiation
ξ – optical thickness,
ρ – density, kgm

Subscripts

ν – vapour phase
m – mixture
0 – stagnation condition

1 Introduction

The experimental research, initiated at the Department of Power Engineering and Turbomachinery (KMiUE) of the Silesian University of Technology at the end of the last century, created an opportunity to supplement knowledge about the phenomenon of steam flow with condensation, tested by numerical fluid mechanics. In parallel with the numerical work, significant progress has been made in experimental studies on the flow of wet steam. Recently, measuring techniques based on recording the phenomenon of extinction of light and ultrasound have been elaborated or improved. In recent years, thermal power plants have requirements to minimize their impact on the natural environment, regardless of the load and parameters of the system. Thanks to the operational experience gained over decades and progress in the field of fluid flow numerical modeling,

stress and strain states modeling in solid bodies, the efficiency of electricity generation in such power units have more than doubled. The current requirements regarding the reduction of pollutant emissions and the flexibility of steam power units, force them to continuously improve operation of the machines and power equipment included in their structure. In the case of steam condensing turbines, which are a key element of, for example, coal-fired, steam-gas or nuclear blocks, an important element for maintenance is the measurement of wetness mass fraction (or dryness) at the turbine outlet. There are many experimental methods used to determine the volume of the liquid phase and, as a result, also wet steam enthalpy in the turbine [32]. Introduction of various types of analyzes of the obtained flow image has now enabled not only the determination of the total value of wet steam wetness but also enabled accurate analysis of its composition. There are currently many measuring methods available for two-phase mixtures, namely impedance [1], optical, electromagnetic or ultrasonic radiation based ones. In the case of tests conducted for opaque factors, there are methods based on Doppler shift of reflected light (laser Doppler velocimetery – LDV), or analysis of shifted images (particle image velocimetry – PIV). Numerous measurement techniques using a laser beam have also been developed. These include Rayleigh scattering [31], Raman spectroscopy [31], laser-induced fluorescence (LIF) [27], spectral spectroscopy [21], as well as techniques using Fraunhofer diffraction of laser radiation by droplets [26], phase Doppler anemometry (PDA) [2] or the use of laser light extinction [6]. Each technique has its advantages and disadvantages and is useful in a specific field of application. Among the methods tested so far, techniques based on the phenomenon of light extinction are of particular interest, attractive due to their relative simplicity of implementation and data interpretation, the possibility of continuous measurement with a quick time response, as well as very limited optical requirements when it comes to access to the measurement space. One of the main techniques currently under development in the application for measurements in steam turbine channels by several significant research centers from Germany [17, 24], China [4, 5] or the Czech Republic [20] is the method based on light absorption, which uses in its basic form the theory of scattering Mie [18] on spherical particles.To determine the basic flow parameters, in addition to knowledge of wetness mass fraction, it is also necessary to know about the thermodynamic parameters of the flowing medium. In the design of the USX probe (ultrasonic and light extinction measuring probe), in addition to measuring pressure and temperature, con-

sideration was given to determining the Mach number in the flow using the ultrasound method. Measurement methods based on technology using the speed of sound propagation in matter, due to the specificity of the interaction, are widely used in many fields of technology, industry and science. They are primarily non-invasive, usually environmentally friendly and can be used externally if access to the test facility is limited. In single-phase flows, knowledge of the speed of sound in a given medium is used to determine critical mass flows or to analyze flow disturbances. Mainly, the speed of sound is required to determine the Mach number, whose knowledge is necessary for the analysis of transonic or supersonic flows. However, the phenomena associated with the lack of homogeneity of the medium or with the thermodynamic imbalance are typical for two- or multi-phase flows. For such conditions, both the mass critical flow and the speed of sound are closely interrelated, greatly complicating the description of occurring phenomena, as well as hindering their correct determination using an experiment. When analyzing the research methods used in the measurement technique of two-phase media, it seems advisable to use an additional method that allows determining flow parameters only from thermodynamic relations and sound velocity in given conditions, while minimizing the size of the measurement area.

2 Condensation phenomenon and elements of light scattering theory

In two-phase flow systems, the typical droplet formation process mainly begins through homogeneous or heterogeneous condensation. Phenomena lead to the creation of the so-called nucleation nuclei, which are a set of molecules that grow under the conditions of the surrounding gas phase. The resulting droplets (primary and secondary) have sizes from 1 μm to 100 μm and high concentrations. The measured moisture content of water vapor as a two-phase mixture is usually determined from the volume fraction of droplets (liquid phase), C_{vl}, and the density of the gas phase, ρ_v, and the liquid phase, ρ_l, in the form

$$y = \frac{m_l}{m_m} = \frac{m_l}{m_l + m_v} = \frac{C_{vl}\rho_l}{C_{vl}\rho_l + (1 - C_{vl})\rho_v}\,, \tag{1}$$

$$C_{vl} = \frac{\pi}{6} D_{32}^3 N. \tag{2}$$

In the last several years, numerical modeling of steam flow with condensation in the final stages of turbines has achieved significant progress [7, 8, 22, 23, 25, 29] and now these methods enable turbine designers and scientists to fully simulate the processes of supercooling, nucleation and droplet growth in the considered area research. However, the current advancement of these methods and the relatively small effort, needed to obtain the results of numerical simulations of condensation of steam flow, often overshadows the fact that the calculations are essentially based on mathematical models, e.g., nucleation and drop growth. As a consequence, at least some of the results of computational fluid dynamics (CFD) must be validated against experimental studies to verify their accuracy.

Such tests are often carried out in laboratory channels with measuring elements in the form of various types of nozzles, in which the steam is continuously expanded from the conditions in the expansion tank installed at the inlet to constant pressure in the outlet chamber, and the condensation process occurs during expansion in the channel. Apart from the instability of the flow, which may result from the occurring heat losses, there are usually no additional disturbances caused, for example, by the presence of blade channels in the actual machine. Also taking into account the fact that, even for nozzle flows, the results of numerical analyzes often differ from the results of experimental tests, especially concerning droplet sizes and their concentration, it is necessary to further confirm the numerical results for flows with steam condensation in turbines using experimental tests. In this regard, it should be mentioned that although the previously determined vapor wetness level is an important parameter for assessing the quality of flow calculations, the droplet size distribution and diameter is the main criterion, since the wetness level itself is usually determined by the thermodynamic conditions at the beginning of the condensation process.

The main scattering parameters, with the use of Mie theory [18], are (Fig. 1):

- wavelength of the incident radiation, λ,
- scattering particle size usually expressed as dimensionless parameter $\left(X = \dfrac{2\pi r}{\lambda}, \text{ where } r \text{ is the radius of the spherical scattering particle}\right)$,
- quantity taking into account optical properties, i.e., the refractive index.

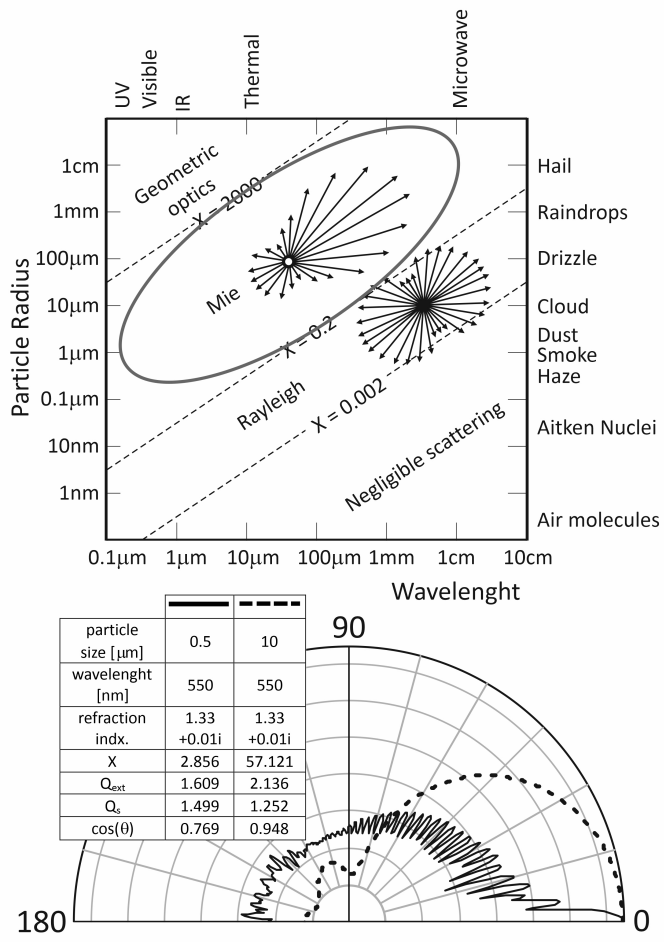

Figure 1: Light scattering regimes and scattering geometry as well as exemplary scattering curves for two different particle diameters (obtained according to the KMiUE procedure).

As can be seen from Fig. 1, in the case of increasing the diameter of the scattering particles, the scattering symmetry changes to increased forward scattering. The main essence is the assumption of particle sphericity and its homogeneity, therefore a single refractive index at a given wavelength can be assumed. For water, the value of the refractive index is usually taken as $n = 1.333$, but this value also depends on the wavelength of the incident light and temperature and in final form must be extended and supplemented.

3 Dependencies regarding the extinction method used in USX probe

In the method of light absorption (extinction), the wavelength, λ, and the original intensity $I_0(\lambda)$ after passing the distance L through the medium of homogeneous particles (drops), is reduced to the intensity $I(\lambda)$ (Fig. 2).

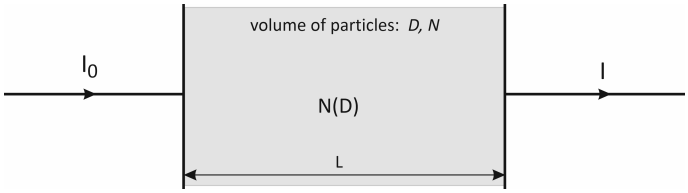

Figure 2: Scheme of attenuation of the primary intensity I_0 after crossing the distance L in the light extinction method.

For the homogeneous distribution of particles, the modified Bouger–Lambert–Beer equation (which is used in absorption spectroscopy) takes the form [32]

$$\frac{1}{t}\ln\left(\frac{I(\lambda)}{I_0(\lambda)}\right) = \frac{\pi}{4}\int_{D_{\min}}^{D_{\max}} Q_{ext}(n, D, \lambda)N(D)D^2\,\mathrm{d}D. \tag{3}$$

In most cases, the Sauter diameter can be used in comparisons, which can be defined as follows for the above considerations:

$$D_{32} = \frac{\int_{D\,\min}^{D\,\max} D^3 N(D)\,\mathrm{d}D}{\int_{D\,\min}^{D\,\max} D^2 N(D)\,\mathrm{d}D}. \tag{4}$$

Figure 3 presents the left side of Eq. (3) graphically, obtaining a curve of the dependence of extinction coefficient from the measurement depending on the wavelength. Then, using the dependencies according to Mie's law, the Q_{ext} coefficient and the final form of the equation can be determined [32]. Knowing the distribution and number of particles, wetness mass fraction can be determined, taking into account thermodynamic parameters of the flowing medium.

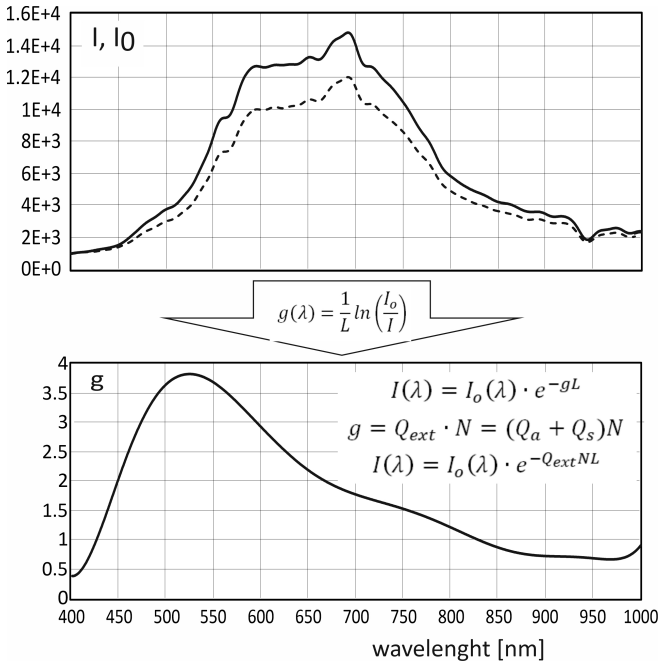

Figure 3: Light intensity curves I and I_0 (KMiUE system – experimental measurement) and the curve of the extinction coefficient g as a function of the wavelength of light.

4 Construction of extinction part of USX probe

Recently, optical methods, based on the technique of light absorption, together with the development of technology, give increasingly accurate and reproducible results. The most important of the advantages of this method can be formulated as follows:

- it is possible to obtain not only information about the wetness level of the steam but also about the size and concentration of liquid phase droplets;
- fiber optic probes are treated rather as non-invasive (or minimally invasive) due to the transparency of the measuring space in which only light is located;
- scattered light data analysis is usually conducted for the visible wave range (0.45–0.80 μm), so you can use simple and relatively cheap optics and spectroscopic systems;

- measurements can be made directly inside the device. No sampling is necessary. Local thermodynamic parameters are not disturbed;
- the measurement is fast, possible to be completed in few seconds or less;
- optical probes can be built into long holders with a circular cross-section with a small outer diameter. Therefore, they can be used to make measurements not only outside the last turbine stage but also between subsequent stages. Such a handle also allows for quite simple integration with the machine structure.

The X probe measuring system at KMiUE (extinction part of USX probe) includes elements of the lighting system in the form of a deuterium-halogen

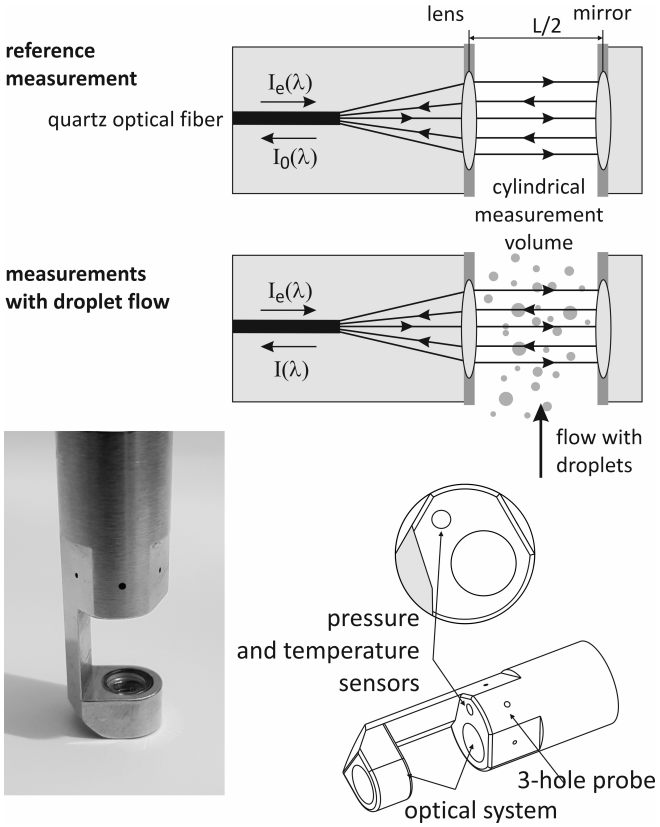

Figure 4: Determination of light extinction coefficient by measurement of reference intensity and attenuated intensity and view of the current version of the X probe.

illuminator and a spectrometer, as well as a traverse system. In addition, probe software was created to automate the measurement process and conduct on-line signal analysis. For the correct determination of the size and number of drops, as well as for a full description of the stream parameters, it is necessary to know the basic thermodynamic parameters of the tested flow. The probe design has implemented a 3-hole probe for measuring several temperatures and pressures, as well as to determine the angle of the flow in relation to the measuring space (Fig. 4).

5 Description of the measuring system

The X probe measuring system (Fig. 5) consists of two main blocks. The first of them is responsible for the production, registration and analysis of the light spectrum, while the second for measurements of thermodynamic parameters. The illuminator used for testing was equipped with two types of light sources enabling the production of a collimated beam both in the visible range (400–1100 nm) and extended to the ultraviolet range (250–400 nm). The fiber optic spectrometer used, manufactured by Optel Opole, is based on a Sony measuring system, which is a CCD (charged-coupled device) ruler with 2048 active elements (pixels) with a 14 bit analog-to-digital (A/D) converter.

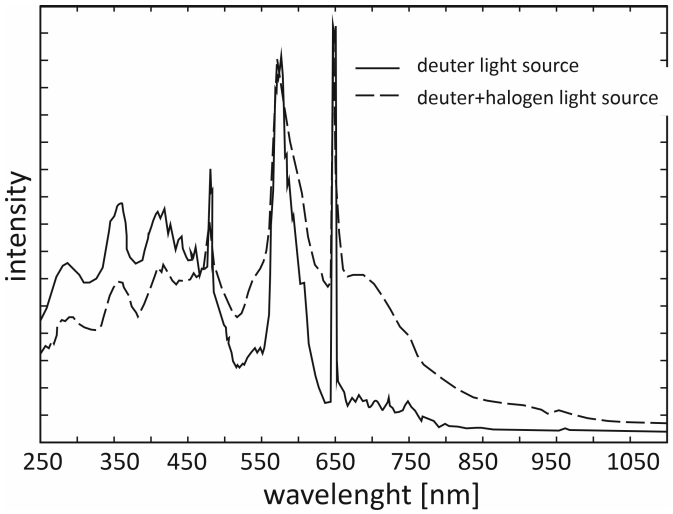

Figure 5: Spectrum of deuterium and deuterium + halogen lamps used in the KMiUE measuring system.

Pressure registration was carried out using high-precision (0.16% FS (full scale)) transducers from Applisens. Due to the minimization of area and resistance to the demanding factor of wet steam, the temperature measurement system is based on calibrated platinum resistance thermometers – PT100 sensors. The test system, prepared and checked for correct operation, was subjected to test and calibration measurements in the medium stream with known droplets diameter and its concentration, as well as in a specially prepared vacuum test chamber. The pressure recording system has been calibrated before being placed in the tunnel following the procedure enabling determination of appropriate calibration factors. The results of the most important tests performed are presented below. Extended information about the test stand and measuring devices can be found in the publication [32] and in the studies of the authors [12, 14, 16].

6 Static and comparative tests of extinction part of USX probe

In the first phase, the values of droplet diameter and their concentration were determined using static tests. For this purpose, polystyrene particles with a diameter $D \cong 2\ \mu\text{m} \pm 0.05\ \mu\text{m}$, $N = 1.2 \times 10^{11}\ 1/\text{m}^3$ suspended in aqueous medium, were used. Figure 6 presents the view of the probe during the tests, as well as the light spectrum I and I_0 along with the graph of particle diameter distribution and their numbers. This figure compares the distribution of the extinction coefficient, $g(\lambda)$ determined during test measurements with the coefficient obtained from the relationship (3). Also, curves showing the relative error ($\pm 5\%$) of the calculated value were marked on the graph. Satisfactory test results for polystyrene particles were achieved, for which the error was 5.75% (2.115 μm – value determined during the test) and the number of particles was 12.1% ($1.06 \times 10^{11}\ 1/\text{m}^3$). The larger error in the number of determined particles could have been caused by the difficulty associated with the correct estimation of their number in the measurement volume. In addition, the test results obtained and the calculation procedure itself was subjected to additional verification, checking them against the procedure developed at the Technical University in Stuttgart (TUS) [17, 24]. The comparative test measurement was based on data obtained from the actual steam flow during tests in the nozzle installed in the steam tunnel. Extensive research on this stand, conducted with the use of wet steam and humid air, has been described in co-author

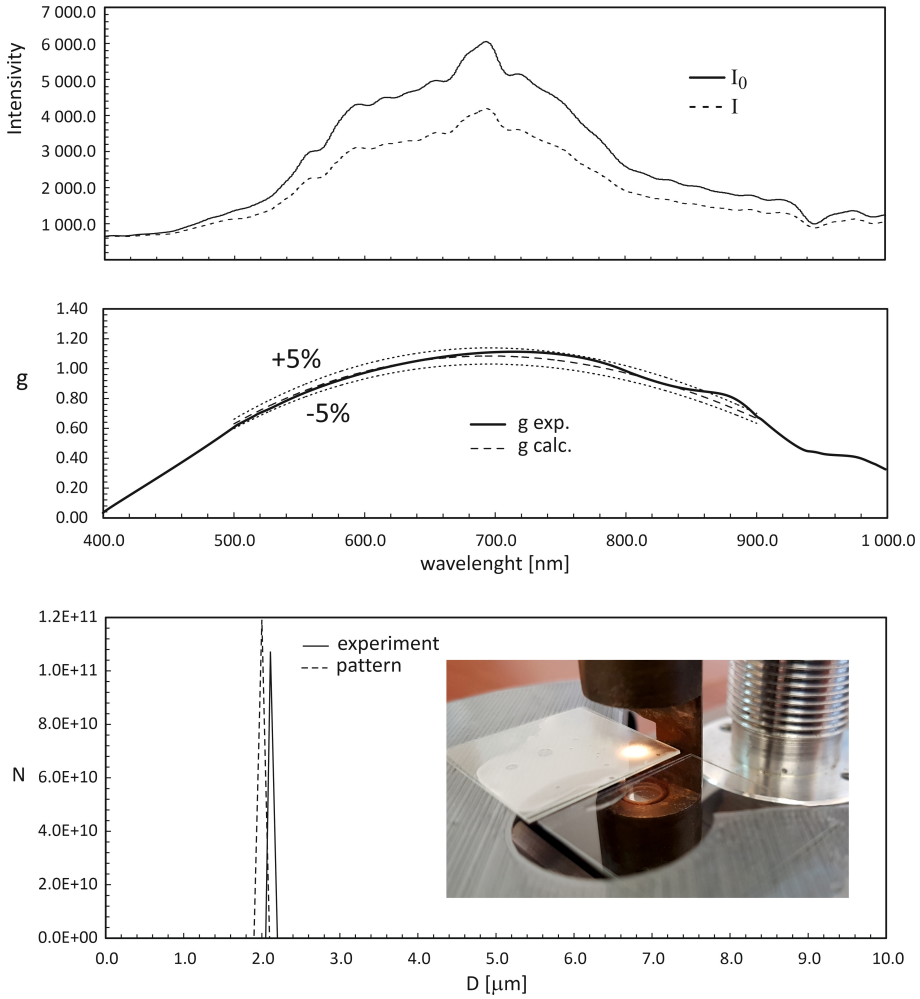

Figure 6: I and I_0 light spectrum, distribution of extinction coefficient g from measurement and calculations, distribution of particle diameter and their number, view of X probe during tests.

monographs [16] and numerous publications [9–13]. For a critical analysis of results, a case was selected for which the results of the comparison of procedures were presented in Fig. 7. Comparative studies have shown high compliance of the proposed calculation procedures. The size deviations determined for the interesting wavelength range of light after optimization of the KMiUE system did not exceed 0.3% for the droplet diameter, and 1.7% for their number, using identical input data.

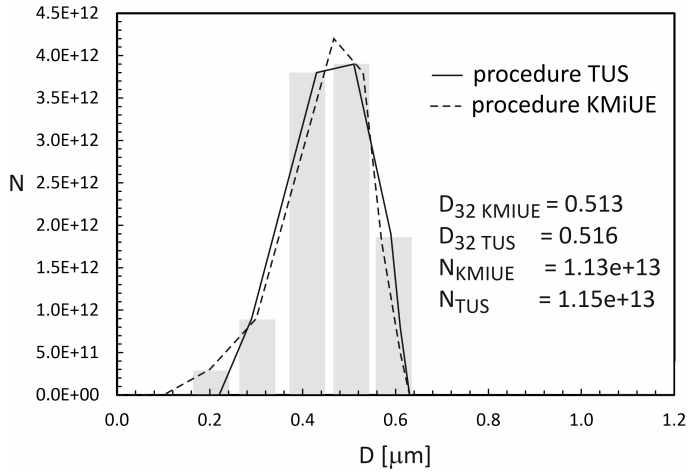

Figure 7: Distributions of droplet diameter and their numbers presented for the KMiUE and TUS procedure.

7 Determination of the wetness and the diameter of the droplets for the real wet steam flow

From the practical application of the presented test method, tests carried out under real conditions of wet steam flow in the steam tunnel give the largest view on its measuring capabilities. The possibility of comparing experimental measurements with advanced numerical fluid mechanics methods carried out in parallel is also valuable. For this purpose, the X probe was used to tests carried out in the research steam tunnel located in the KMiUE Thermal Machinery Hall, used for a wide spectrum of steam flow tests, using various types of nozzles and blade channels. Research using the installation has been extensively described in publications over the last several years [14–16]. To carry out the tests, a measuring nozzle with the geometry shown in Fig. 8 [14], and the commercial software were used.

Numerical modelling was carried out using an in-house CFD code as well as the commercial code Ansys CFX [19]. For both applied CFD codes th numerical simulation was based on time-dependent 3D Reynolds averaged Navier-Stokes equations (RANS equations). Together with mass, momentum and energy conservation equations formulated for the vapour/water mixture (single-fluid model), two equations for the shear stress transport (SST) turbulence model and three additional transport equations for the

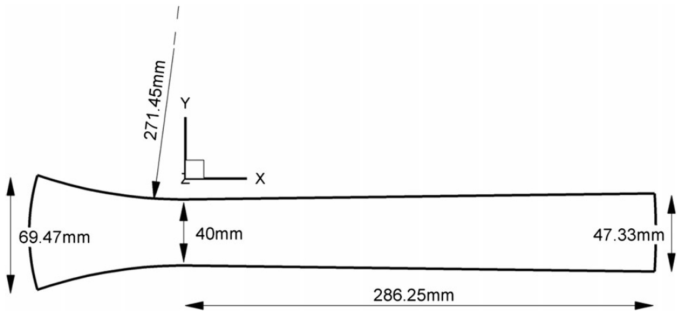

Figure 8: The geometry of the measured nozzle [14].

liquid phase are solved. For the two-phase nonequilibrium flow it is assumed that the volume occupied by droplets is negligibly small. The models does not take account of the interaction between droplets. The heat exchange between the liquid phase and the solid boundary, as well as the velocity slip between the vapour and the liquid phase are neglected [30]. The obtained results of numerical analyzes were compared with the results obtained at the laboratory, i.e. with the distribution of static pressure along with the nozzle, the image of the flow field obtained using the Schlieren technique and, most importantly, with the measured wetness and the Sauter diameter, determined at the outlet of the measuring nozzle. A more detailed description of the experimental research object and the complementary measuring techniques used in the experiment were presented in [3, 10, 12]. Two measurement series were selected for analysis from many sessions of conducted tests. They differ in the total temperature at the inlet of the nozzle, at almost the same total pressure. In the first case, the values at the nozzle inlet are $p_0 = 124$ kPa and $t_0 = 118$ °C, in the second case $p_0 = 128$ kPa and $t_0 = 121$ °C. For the first case (Fig. 9a), comparing the wetness mass fraction and the average droplet size from measurements, concerning both numerical codes, it can be observed that both determined values are higher than the values determined by Ansys CFX program and calculated by own numerical code developed at KMiUE. Similar relationships can be seen in the second selected case (Fig. 9b). Although for the degree of humidity the results of numerical tests and the experiment are quite similar, in the case of the Sauter diameter, the results of the experiment are about 50% higher, compared to the results of numerical calculations. However, even the results of two numerical analyzes alone in an interesting area show significant differences in

the values of the obtained quantities. Although the tests performed in real flow conditions did not give significant results of quantitative tests, they showed additional technical and measuring imperfections of the constructed probe.

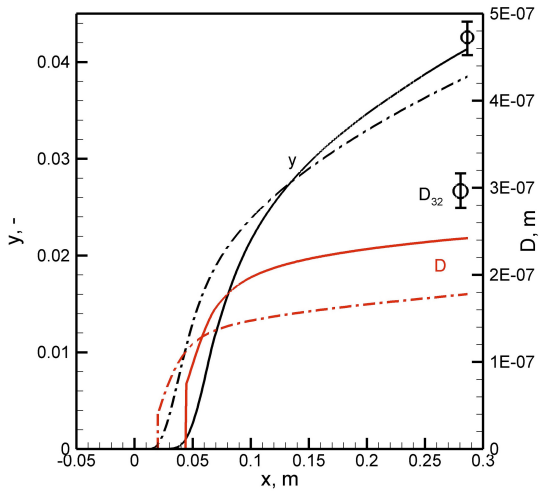

(a)

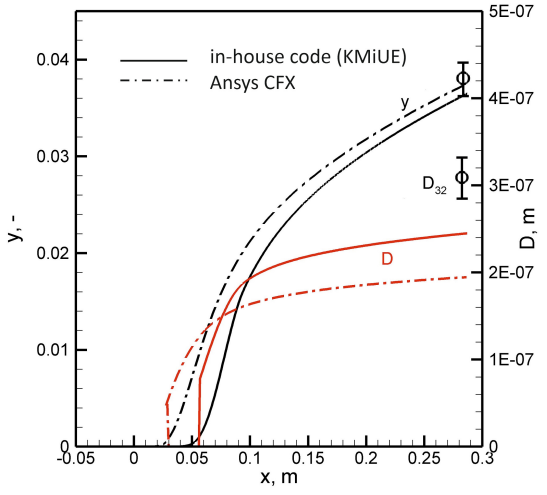

(b)

Figure 9: The comparison of the wetness mass fraction, y, and the average droplet size, D, from measurements with numerical results. Liquid phase parameter distribution along the nozzle for (a) $p_0 = 124$ kPa, $t_0 = 118$ °C and (b) $p_0 = 128$ kPa, $t_0 = 121$ °C with Sauter mean diameter D_{32} and y.

8 The basic principle of sound velocity for two-phase medium

The complex interactions of the ultrasonic wave with the test medium generally include various forms of scattering, absorption, reflection and diffraction. In [35], the author divided the propagation of ultrasonic waves in media containing a liquid phase into three categories, depending on the relationship between the droplet size and the length of the ultrasonic wave (Fig. 10). A distinction is made here between the category designated LWR for low wave frequency region, IWR for medium and SWR for high frequency region. Considering typical droplet sizes for wet steam or humid air applications (0.1–10 μm), occurring when the ultrasonic technique of the output signal frequency is used, they are in the LWR range (0.1–100 MHz). Ultrasounds, as mechanical disturbances of the medium, spread through a given medium at a constant temperature at a constant speed. Because propagation at the molecular level occurs due to interactions between the molecules, the speed at which the wave propagates depends on the mass of the molecules, their distance and the forces of intermolecular attraction. The speed of sound in gases depends on the temperature. The higher the gas temperature, the faster its molecules move and the higher the speed of sound is. The relationship taking into account changes in gas parameters

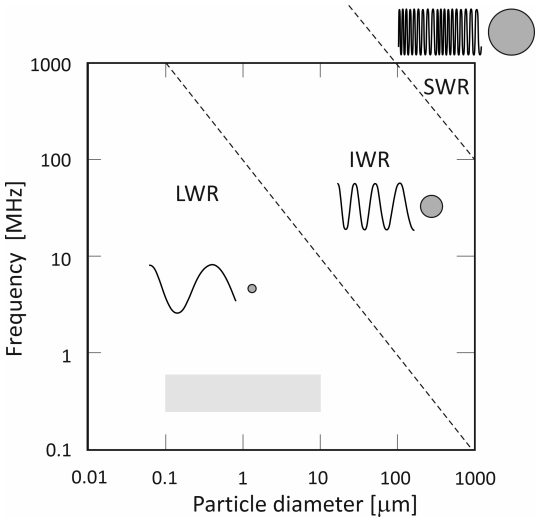

Figure 10: Relationship between droplet size and ultrasonic wavelength frequency (LWR, IWR, SWR – low, intermediate, and high frequency region).

for perfect gases during the adiabatic conversion can be determined from the basic pressure formula

$$p = \frac{p_0 V_0^{\kappa}}{V^{\kappa}} \,. \tag{5}$$

The speed of sound wave propagation in gases can be described as

$$c^2 = \left.\frac{\partial p}{\partial \rho}\right|_s \,. \tag{6}$$

When considering two-phase flows, assuming first the homogeneity of the phases and the lack of friction between them, the specific volume can be expressed as

$$\frac{1}{\vartheta} = \frac{1}{\vartheta_a \left(1 - y_{\max}\right) + \vartheta_l y_{\max}} \tag{7}$$

or for density:

$$\frac{1}{\rho} = \frac{\left(1 - y_{\max}\right)}{\rho_a} + \frac{y_{\max}}{\rho_l} \,. \tag{8}$$

By differentiating the above equation concerning pressure at a constant moisture content (mass fraction of a liquid phase)

$$\frac{1}{\rho^2}\frac{\partial \rho}{\partial p} = -\frac{\left(1 - y_{\max}\right)}{\rho_a^2}\frac{\partial \rho_a}{\partial p} - \frac{y_{\max}}{\rho_l^2}\frac{\partial \rho_l}{\partial p} \,, \tag{9}$$

hence

$$\frac{1}{\rho^2}\frac{1}{c^2} = -\frac{\left(1 - y_{\max}\right)}{\rho_a^2}\frac{1}{c_a^2} + \frac{y_{\max}}{\rho_l^2}\frac{1}{c_l^2} \,. \tag{10}$$

Similarly, the above equation can be expressed by the volume fraction α, multiplying by the density of the media. The volume fraction for the air-water mixture case is better in describing the sound velocity of the mixture because it omits the huge difference in the density of both phases:

$$\frac{1}{\rho^2}\frac{1}{c^2} = -\frac{\left(1 - y_{\max}\right)}{\rho_a^2}\frac{1}{c_a^2} + \frac{y_{\max}}{\rho_l^2}\frac{1}{c_l^2} \,. \tag{11}$$

Considering steam as a medium, determining the speed of sound from the relationship (6) is too simplified. It is obvious that due to the much more complex equation of state for water vapor, presented for example in the formulations of the International Association for the Properties of Water and Steam (IAPWS) [34], this approach is incorrect. However, it should be mentioned that usually, sound velocity measurement data are only available

for single-phase factors. Examples of determining this magnitude for the wet steam area can be found [36, 39], but they usually end in the area of numerical simulations and to the author's knowledge no experimental data have been presented in the literature. As described in [38], based on IAPWS, the speed of sound for steam depending on pressure and temperature can be expressed dimensionless as

$$c(\pi,\tau) = \sqrt{\frac{RT\left(\dfrac{\partial\gamma}{\partial\pi}\right)^2\tau^2\dfrac{\partial^2\gamma}{\partial R^2}}{\left(\dfrac{\partial\gamma}{\partial\pi}-\tau\dfrac{\partial^2\gamma}{\partial\pi\partial\tau}\right)^2-\dfrac{\partial^2\gamma}{\partial\pi^2}\tau^2\dfrac{\partial^2\gamma}{\partial R^2}}}, \tag{12}$$

where: $\pi = p/p_k$ – reduced pressure, $\tau = T_k/T$ – reduced thermodynamic temperature, $\gamma(\pi\tau) = g(p,T)/RT$ – dimensionless function determined from the Gibbs energy equation, R – Boltzmann (gas) constant, T – thermodynamic temperature, the subscript k indicates critical parameters given according to IAPWS for water ($T_k = 647.096$ K, $\rho_k = 322$ kg/m^3). These relationships according to [37] are presented graphically in the drawing (Fig. 11).

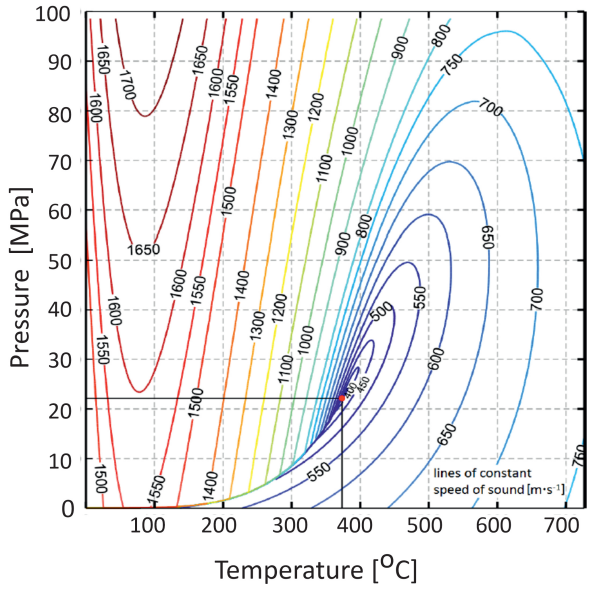

Figure 11: Values for the speed of sound in water and steam in a p-T diagram [37].

In the calculations of sound speed presented in [37], one can see the quite good agreement of the analyzes carried out, both for superheated and saturated steam with IAPWS data. The state parameters, for a two-phase medium, are defined according to Maxwell's equations as equilibrium parameters. From a thermodynamic point of view, wet steam at equilibrium is therefore considered a continuous mixture that contains both phases (water and saturated steam) depending on the degree of dryness. The speed of sound obtained in this state can, therefore, be referred to as equilibrium sound speed and calculated similarly for the entire wet steam area.

9 Determination of physical quantities by ultrasound method

The ultrasonic method is based on the physical relationship between the speed of propagation of ultrasonic waves in a given medium and the specificity of that medium. The main problem in the ultrasonic method adopted in the USX probe application is the estimation of the so-called time-of-flight (TOF). TOF is the time between the beginning of the generation (sending) of the pulse from the transmitter and the beginning of the echo signal recorded in the receiver, as a result of e.g. discontinuities in the propagation medium. The simple formula can be used when it is necessary to determine the sound speed in a given medium as the desired value:

$$c = \frac{L}{\mathrm{TOF}} \,. \tag{13}$$

In this case, it is necessary to very accurately determine the distance L (direct measurement) between the transmitter and receiver (Fig. 12). It is also necessary to know the structure of the transducer itself and the geometrical position of the elements sending and receiving sound waves. Figure 13 shows an example of a recorded signal with the location of the signal start point and TOF. In the trough transmision (TT) method, the analyzed area is located between two transducers that act as a transmitter and receiver (Fig. 12). The transmitter generates a pulse that travels through the test area and is registered by the receiver. In the measurement of substances (e.g. multiphase systems, emulsions, etc.), where it is also important to determine the distribution of droplets and their diameters, very often, in addition to determining the speed of sound from the recorded signal, the coefficient of signal weakening after passing through the sample is

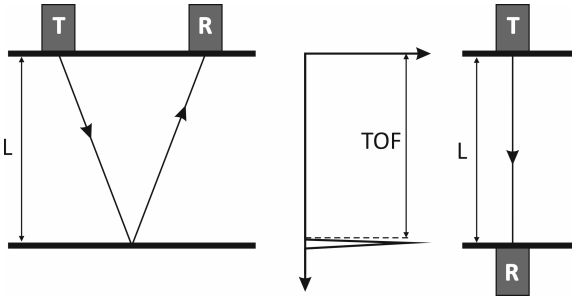

Figure 12: Waveforms of ultrasound wave and examples of signals observed using through-transmission method, with L and TOF values; L – distance, T – transmitter, R – receiver, TOF – time-of-flight.

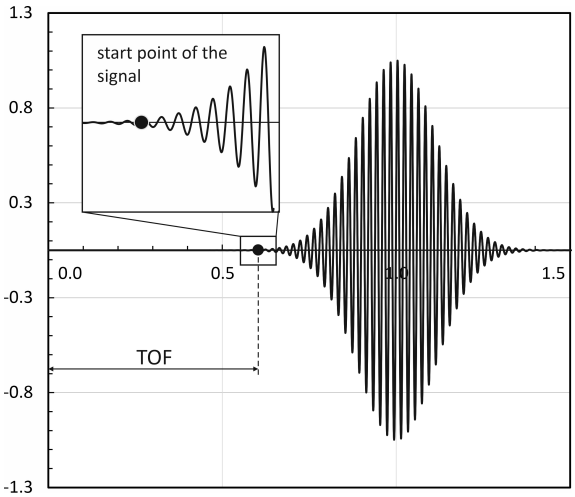

Figure 13: TOF location in ultrasonic measurement.

also calculated. Both quantities are obtained from the knowledge of TOF and the signal amplitude for the tested medium. The attenuation factor is usually calculated from the change in the amplitude of the transmitted and received signal, comparing it to the material factor for which it is known. In this case, the measurement is usually made only for a signal with one known frequency or narrow range. Detection of the entire range of changes usually also requires scanning of the measuring area for different frequency values. Although the basics of this measurement are fairly simple, there are a few problems to consider in determining the TOF size correctly. One of the most important is the temperature dependence of the TOF size, i.e.

ensuring uniformity and invariability of the temperature of the measuring volume during the tests. Also, the possibility of acoustic reflections or reverberations may cause a significant weakening of the amplitude or the appearance of a large amount of noise in the signal. Considered should also be the effects of ultrasonic wave diffraction and phase shifts, which have their basis even in not fully parallel shields. The figure (Fig. 14) shows a typical schematic view of the TOF determination measuring system using a TT type system.

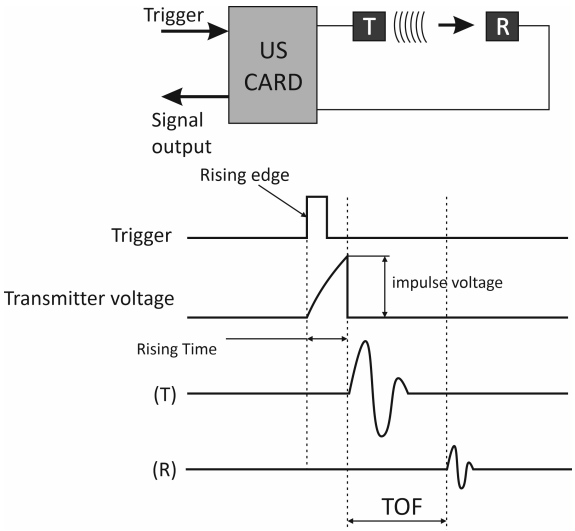

Figure 14: Diagram of the TT type measurement system.

In order to test the correct operation of the systems used, tests were carried out to determine the directional characteristics of the sensors and their maximum signal, which is important in testing the flow of gases with higher flow velocities. Because the sensors can also be mounted not only in the point probe but also in opposite walls of the flow tunnels, the signal attenuation characteristics along with the distance were determined to select the appropriate minimum and maximum distance from the transmitter to the receiver. The tests were carried out with water as a medium at a constant temperature of 23 °C, using a system constructed for this purpose, enabling precise mutual positioning of the sensors. Figure 15 presents examples of directional characteristics of the sensors used, recorded in the (Fig. 15a, b) horizontal (0°) and vertical (90°) axes of the sensor. Indications are given as relative values related to the registered maximum amplitude. The graphs

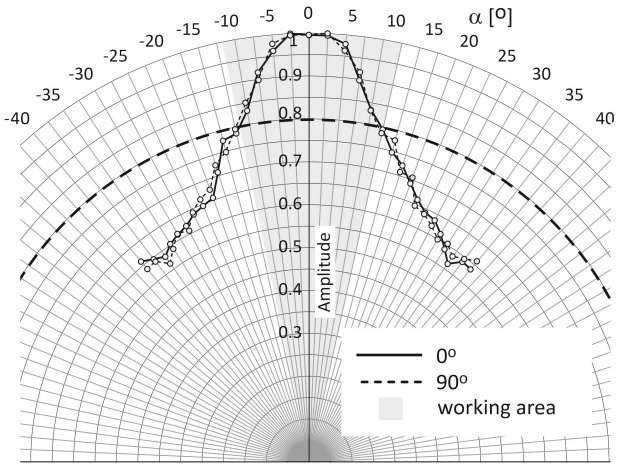

(a)

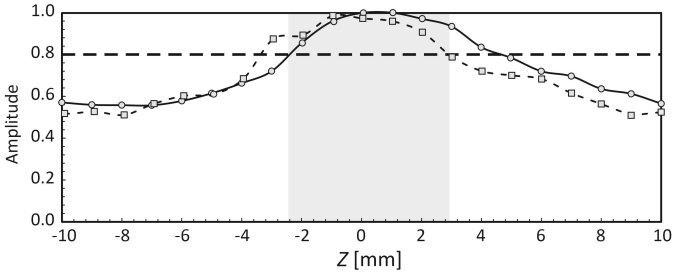

(b)

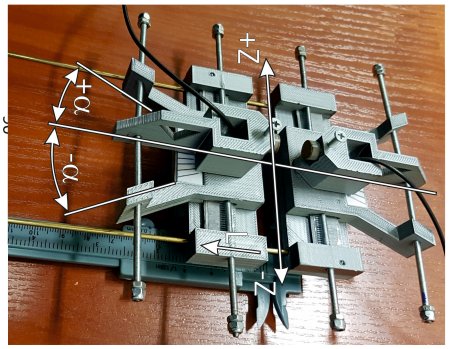

(c)

Figure 15: Directional characteristics of the applied ultrasonic sensors: a) α angle changes for two axes of the sensor settings – horizontal (0°) and vertical (90°; b) Z distance changes for two axes of the sensor settings – horizontal (0°) and vertical (90°), c) designation of parameters changed during the tests.

also indicate the proposed range of sensors for 20% signal attenuation. As can be seen for both graphs (Fig. 15a), the characteristic shows good directional consistency in the whole range of measured angles (α). It can also be seen that correct indications with maximum signal amplitude are possible to obtain for the sensors used only within an angle range of $\pm 12^{\circ}$. This is a fairly typical operating range of this type of ultrasonic sensor. However, for factors with high attenuation, it is advisable to position the transmitter and receiver in the range of $\pm 3^{\circ}$ as much as possible (Z-axis) to maximize the measured signal amplitude. Similar relationships were observed in Fig. 15b, in which the curve depicting the shift of the axis of the transmitter and receiver in the range of ± 10 mm concerning each other was placed.

10 Ultrasound measuring system

Figure 16 shows a block diagram of the system used to support the constructed US probe. In the first place, only the ultrasonic part itself was tested.

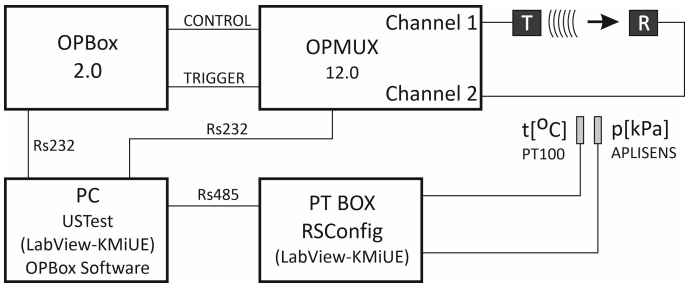

Figure 16: Block diagram of the US probe measuring system.

The system consists of a miniature ultrasonic data acquisition device with integrated pulse transmitter OPBOX 2.1, Optel sp.z o.o, cooperating with the mixer OPMUX 12.0, as well as it's own (KMiUE) automated measuring and control system PTBOX. The whole system is controlled using a PC and serial communication devices RS-232 and RS-485, first with the standard OPBOX software program supplied with the system, and then, to extend the possibility of sampling and analysis of the signal, using its own USTest software (Fig. 16) programmed in the LabView environment. The system also includes two pairs of piezoceramic ultrasonic transducers with a frequency of 0.450 MHz. The OPBOX system has a measuring band of 0.5–25 MHz and a controlled range of filters in 16 different measuring ranges.

The measurement data acquisition system has been designed for performing real-time acquisitions at a speed of up to 10 kS/s. The system can work with four transducers operating separately as a transmitter or receiver. In the conducted tests, the signal analysis and, in the end, the procedure of determining the TOF was carried out according to the algorithm presented in Fig. 17. Determination of the TOF to critically compare the results obtained was carried out in several ways known from the literature, however, for the final analysis, the method of determining the approximation curve was chosen, from the envelope points of the noisy signal, the intersection of which with the time axis will constitute the TOF sought.

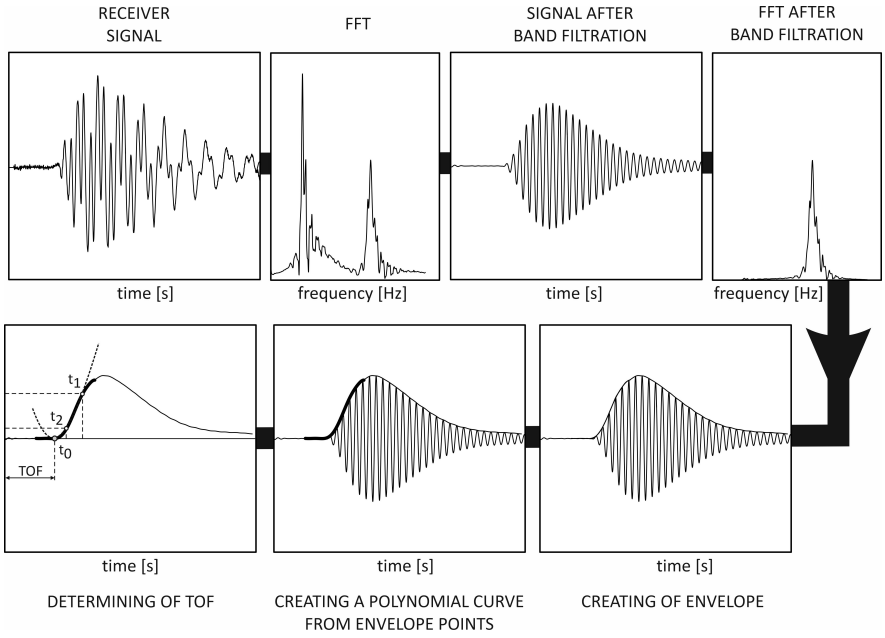

Figure 17: Ultrasonic signal analysis procedure applied in the measuring stand.

11 Determination of parameters for the real signal conditions for ultrasound part of USX probe

First, the parameters were determined and the procedure presented in Fig. 17 for the simulated signal was checked [32]. In the next phase, the

test method used and the constructed measuring system was tested in real conditions. For this purpose, a test system was installed which allows determining the value of sound velocity depending on the temperature for water and air at atmospheric pressure. A sound speed dependence curve was determined depending on the water temperature. The values of sound velocity determined in the process of testing along with the relative error depending on the temperature range from 8–90 °C, are presented in Fig. 18 in the form of a graph. For comparison, as a standard for the speed of sound, values determined from the dependencies given in [33]. Observing the curves on the graph, the good agreement of the result of experiment with theoretical data can be observed. In the whole range of temperature changes, the relative time error is within ±0.5% (dashed lines).

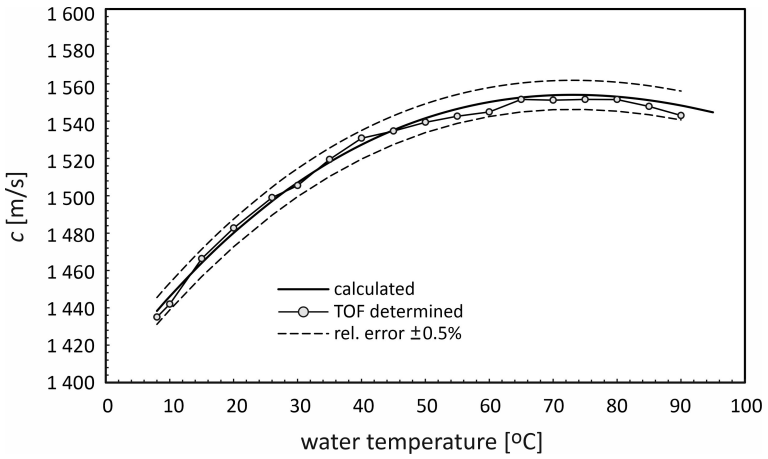

Figure 18: The sound velocity values for water along with the total error depending on the water temperature range from 8–90 °C.

After the procedure carried out, the correctness of the method used was found for most of the experimental data. The SNR (signal-to-noise ratio) level proved to be extremely important here, which in the case of the method used in KMiUE should be greater than about 1–2 dB so that it is possible to correctly isolate the echo signal from the measured noisy signal. In the case of higher levels of noise, obtaining the correct TOF time is also possible, but the measurement should be carried out with averaging the signal over time, and the procedure requires the use of manual selection of analysis parameters.

12 Proposed construction of a comprehensive USX probe

After various tests, an attempt was made to create a prototype design of the USX probe combining both measuring methods, the extinction method, and the ultrasonic method as well as other measuring sensors allowing to determine the necessary thermodynamic parameters of the flow [32]. The proposed construction solution is shown in Fig. 19. As can be seen in the figure, the X-shaped intersecting beam system was used for both measuring volumes. Due to the size of the sensors and optics used in the KMiUE solution, the probe must have a diameter of about 20 mm. However, in typical tunnels and turbine ducts, this value is satisfactory for measurements with low error. At present, the USX probe, and especially its ultrasonic version, is still in the phase of preliminary experimental research aimed at checking its indications in conditions of steam flow.

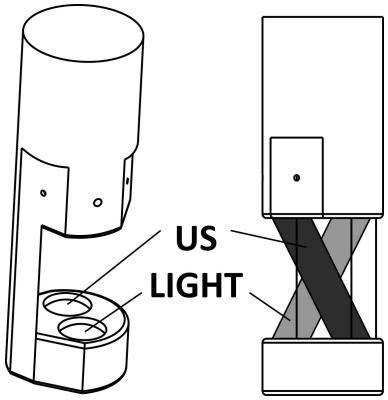

Figure 19: Proposed construction of KMiUE USX probe.

13 Conclusions

The aim of the work was to develop a proprietary measurement procedure for a comprehensive method for determining the parameters of two-phase flow occurring in power machines mainly the flow of wet steam in steam turbines. The basic value, determined experimentally in the final phase, was the content of the liquid phase, defined as the wetness mass fraction of the medium. The design and testing procedure was described, as well as the tests in real conditions of the own USX probe. For the probe, both

static and dynamic tests were carried out at specially designed test stands. A comparative analysis of the correctness of the calculation method was carried out. Test results show that this method has good repeatability and reliability of obtained results under static conditions. For the extinction part of the probe, errors in determining the Sauter diameter are in the range of 5.75% and the number of particles 12.1%, which was considered good values for this type of measuring instruments, comparable to the error size of similar systems developed in other research centers. A calibration and functional check of the other temperature and pressure sensors included in the probe head were also carried out. In this case, it was also found that the flow velocity and angles were determined correctly, as well as the temperature values. During tests in real flow, the experiments showed the possibility of using the constructed probe for wet steam flow tests, the need to refine the mechanical design of the probe was noticed, and a slight discrepancy was obtained in the values obtained from the numerical analysis. However, it should be stated that both the results of real and static tests show that the developed measuring system is capable of measuring online the moisture content of steam in the KMiUE laboratory steam tunnel as well as the low-pressure steam turbine. In developing the design of the US probe, the main challenge (due to the accuracy and repeatability of the obtained sound speed results, and thus also the determined wetness mass fraction) was to obtain a precise TOF of the recorded signal. Proprietary modifications of TOF determination methods were proposed and they were checked by analyzing various types of simulation signals obtained from mathematical relationships. Preliminary tests were also carried out, during which it was found that the sensors used were very useful in the case of water and weaker to obtain satisfactory results for humid air. At the current stage of probe development, it is still difficult to determine its usefulness for testing steam flow due to the appearing large dispersion of the ultrasonic signal along with the increasing wetness of the medium.

Acknowledgements The presented results were performed within the project TANGO 3 08/050/TAN19/0200 of The National Centre for Research and Development and Statutory Research Funds of the Silesian University of Technology.

Received 24 April 2020

References

[1] Andreussi P., Di Donfrancesco A., Messia M.: *An impedance method for the measurement of liquid hold-up in two-phase flow*. Int. J. Multiphas. Flow **14**(1988), 777–785.

[2] Bachalo W.D., Houser M.J.: *Phase Doppler spray analyzer for simultaneous measurements of drop size and velocity distributions*. Opt. Eng. (1984), 583–890.

[3] Blaszczuk A.: *Experimental investigation of natural convection inside a upper part of vertical converging air channel using the Schlieren technique*. Exp. Thermal Fluid Sci. **50**(2013), 178–186.

[4] Cai X.S., Wang N.N., Wei J.M., Zheng G.: *Experimental investigation of the light extinction method for measuring aerosol size distributions*. J. Aerosol Sci. **23**(1992), 7, 749–757.

[5] Cai X., Wanc L., Ouyang X., Pan Y.: *A novel integrated probe system for measuring the two phase wet steam flow in steam turbine*. J. Eng. Thermophys. **22**(1992), 6, 52–57.

[6] Dobbins R.A., Jizmagia G.S.: *Particle size measurements based on use of mean scattering cross sections*. J. Opt. Soc. Am. (1966).

[7] Doerffer P., Dykas S.: *Numerical analysis of shock induced separation delay by air humidity*. J. Therm. Sci. **14**(2005), 2, 120–125.

[8] Dykas S.: *Numerical calculation of the steam condensing flow*. TASK Quart. **5**(2001), 4, 519–535.

[9] Dykas S., Majkut M., Smołka K., Strozik M.: *Research on steam condensing flows in nozzles with shock wave*. J. Power Technol. **93**(2013), 5, 288–294.

[10] Dykas S., Majkut M., Smołka K., Strozik M.: *Experimental research on wet steam flow with shock wave*. Exp. Heat Transfer **28**(2015), 5, 417–429.

[11] Dykas S., Majkut M., Smołka K., Strozik M.: *Analysis of the steam condensing flow in a linear blade cascade*. Proc. Inst. Mech. Eng., A J. Power Energy **232**(2018), 5, 501–514.

[12] Dykas S., Majkut M., Strozik M., Smołka K.: *Experimental study of condensing steam flow in nozzles and linear blade cascade*. Int. J. Heat. Mass Tran. **80**(2015), 50–57.

[13] Dykas S., Majkut M., Strozik M., Smołka K.: *Non-equilibrium spontaneous condensation in transonic steam flow through linear cascade*. In: Proc. 11th European Conf. on Turbomachinery (2015), ID: ETC2015-047.

[14] Dykas S., Majkut M., Strozik M., Smołka K.: *An attempt to make a reliable assessment of the wet steam flow field in the de Laval nozzle*. Heat Mass Transfer **54**(2018), 2675–2681.

[15] Dykas S., Majkut M., Strozik M., Smołka K.: *Comprehensive investigations into thermal and flow phenomena occurring in the atmospheric air two-phase flow through nozzles*. Int. J. Heat Mass Tran. **114**(2017), 1072–1085.

[16] Dykas S., Smołka K., Majkut M., Strozik M.: *Analysis of the thermal flow phenomena in transonic flows of moist air in nozzles*. Publ. House Silesian Univer. Technol., Gliwice 2018 (in Polish).

[17] Eberle T., Schatz M.: *Experimental study of droplet size and wetness in a model steam turbine using light extinction measurements*. In: Proc. 25th Turbomachinery Workshop, Gdańsk/Krzeszna 2011.

[18] Horvath H.: *Gustav Mie and the scattering and absorption of light by particles: Historic developments and basics*. J. Quant. Spectrosc. RA **110**(2009), 787–799.

[19] Ansys CFX Theory Guide (2017) ANSYS 17.1.

[20] Kolovratník M., Bartoš O.: *CTU Optical probes for liquid phase detection in the 1000 MW steam turbine*. EPJ Web of Conf. **92**(2015), 02035.

[21] Ma L., Sanders S.T., Jeffries J.B., Hanson R.K.: *Monitoring and control of a pulse detonation engine using a diode-laser fuel concentration and temperature sensor*. Proc. Combust. Inst. **29**(2003), 161–166.

[22] Puzyrewski R.: *Theoretical and experimental studies on formation and growth of water drops in LP steam turbines*. Trans. Inst. Fluid-Flow Mach. 42–44(1969), 289–303.

[23] Puzyrewski R., Gardzilewicz A., Baginska M.: *Shock waves in condensing steam flowing through a Laval nozzle*. Arch. Mech. **25**(1973), 3, 393–409.

[24] Schatz M., Eberle T.: *Experimental study of steam wetness in a model steam turbine rig: presentation of results and comparison with computational fluid dynamics data*. Proc. IMechE A: J Power Energy **228**(2014), 2, 129–142.

[25] Wróblewski W., Chmielniak T., Dykas S.: *Models for water steam condensing flows*, Arch. Thermodyn. **1**(2012), 9, 67–86, doi: 10.2478/v10173-012-0003-2.

[26] Swithenbank J., Beer J.M., Taylor D.S., Abbot D., McCreath G.C.: *A laser diagnostic technique for the measurement of droplet and particle size distribution*. Prog. Aeronaut. Astronaut. **53**(1977), 421–447.

[27] Thurber M.C. and Hanson R.K.: *Simultaneous imaging of temperature and mole fraction using acetone planar laser-induced fluorescence*. Exp. Fluids **30**(2001), 93–101.

[28] Twomney S.: *On the numerical solution of Fredholm integral equations of the first kind by the inversion of the linear system produced by quadrature*. J. ACM (JACM) **10**(1963), 1, 97–101.

[29] White A.J.: *Condensation in steam turbine cascades*. PhD thesis, University of Cambridge, Cambridge 1992.

[30] Wróblewski W., Dykas S., Gepert A.: *Steam condensing flow in turbine channels*. Int. J. Multiphase Flow **35**(2009), 6, 498–506.

[31] Zhao H. and Ladommatos N.A.: *Optical diagnostics for in-cylinder mixture formation measurements in IC engines*. Prog. Energ. Combust. **24**(1998), 297–336.

[32] Majkut M.: *Advanced techniques of experimental research and visualization of the compressible gas flow in power engineering machinery*. Publ. House Silesian Univer. Technol., Gliwice 2019 (in Polish).

[33] Bilaniuk N., Wong G.: *Speed of sound in pure water as a function of temperature*. J. Acoust. Soc. Am. **93**(1993), 3, 1609–1612.

[34] *IAPWS Revised release on the IAPWS industrial formulation 1997 for the thermodynamic properties of water and steam*, IAPWS Release 2007.

[35] McClements D.J.: *Principles of ultrasonic droplet size determination in emulsions.* Langmuir **12**(1996), 14, 3454–3461.

[36] Petr V.: *Wave propagation in wet steam.* J. Mech. Eng. Sci. C **218**(2004), 871–882.

[37] Šafaříka P., Novýb A., Jíchaa D., Hajšman M.: *On the speed of sound in steam.* Acta Polytech. CTU Praque **55**(2015), 6, 422–426.

[38] Wagner W., Cooper J.R., Dittmann A., Kijima J., Kretzschmar H.-J., Kruse A., Mareš R., Oguchi K., Sato H., St'ocker I., Šifner O., Takaishi Y., Tanishita I., Trübenbach J., Willkommen Th.: *IAPWS industrial formulation 1997 for the thermodynamic properties of water and steam.* J. Eng. Gas Turb. Power **122**(2000), 150–182.

[39] Young J. B., Guha A.: *Normal shock-wave structure in two-phase vapor-droplet flows.* J. Fluid Mech. **228**(1991), 243–274.